SAND2025-02983J

Binding of Sulfates and Water to Monovalent Cations

Mark J. Stevens* and Susan B. Rempe*

Center for Integrated Nanotechnologies, Sandia National Laboratories, Albuquerque, NM, 87185

E-mail: msteve@sandia.gov; slrempe@sandia.gov

Abstract

The binding of the sulfate ligand group to monovalent cations in the presence of water is important for many systems. To understand the structure and energetics of sulfate complexes, we use density functional theory to study ethyl sulfate binding to the monovalent cations, Li^+, Na^+ and K^+, and to water. The free energies of binding and optimal structures are calculated for a range of the number of ethyl sulfates and waters. Without water, the most optimal structure for all the cations is bidentate binding by two ethyl sulfates, yielding a four-fold coordination. With water, the lowest free energy structures also have two ethyl sulfates, but the coordination varies with cation. For complexes with water, the four oxygen atoms in the sulfate group enable multiple binding geometries for the cations and for hydrogen bonding with water. Many of these geometries differ in free energy by only a small amount (1-2 kcal/mol), meaning there will be multiple binding configurations in bulk solution. In comparison to the optimal structures for binding to the carboxylate group, there is more variation for binding to the sulfate group as a function of cation type and number of waters. Polarization of the atoms is significant and varies among the sulfate oxygen atoms. The water oxygen charge is often larger than sulfate oxygen, which plays a role in the preference for monodentate ligand binding to cations in the presence of water.

Introduction

The interaction of monovalent cations with the sulfate ligand in water is broadly important for a wide range of molecular systems.[1,2] The addition of sulfate groups to macromolecules is a common mechanism to make them soluble in water. Thus, multiple whole classes of polymers and other macromolcules are sulfated. For example, many commercial detergents incorporate sodium dodecyl sulfate.[3] While the sulfate group is not part of the base of biomolecules, such as nucleic acids, proteins, and lipids, there are several classes of biomolecules that are sulfated by enzymes and have important biological functions.[2] For example, sulfate monoesters also play a central role in cell signaling functions.[3] Furthermore, several classes of sulfated compounds occur in humans and other vertebrates.[2] These include cerebrosides sulfates, steroid sulfates and glycosaminoglycans (GAG). The GAGS are major structural constituents of the extracellular matrix and participate in numerous physiological processes. In particular, one GAG, keratan sulfate, is widely distributed in the extracellular matrix of cornea, bone, cartilage, brain, and on the surface of epithelial tissues.[4] In fact, sulfate groups occur on many glycosaminoglycans (GAGs), modulating extracellular signals such as cell–cell and cell–matrix interactions.[5] Diseases associated with errors in GAG sulfation include Alzheimers and cancer. Thus, understanding the basic cation interaction with the sulfate group is relevant for a wide variety of biological systems.

Sulfates have received less theoretical treatment than other charged ligands, like carboxylates. Because the electrostatic interactions in the sulfate systems mentioned above can involve strong polarization and/or charge transfer, density functional theory (DFT) is an appropriate theoretical approach to study sulfates. Most calculations have treated a single sulfate binding to a single anion or water. Previous DFT calculations of sulfate include treatment of methyl and ethyl sulfates.[6] Prior studies mostly characterized the structure of methyl and ethyl sulfate molecules with treatment of a single water binding to the methyl sulfate using a self-consistent field method with the 6-31+G** basis set. DFT calculations of alkyammonium-alkylsulfate complexes were carried out by Aleman et al.[7] They performed calculations in the gas phase up to the MP2/6-311++G(d,p) level of theory, and investigated the influence of the bulk solvent at the HF/6-311++G(d,p) level using the polarizable continuum model. Remko et al. performed DFT calculations for Li^+ and Na^+ binding to carboxylate, sulfate and phosphate complexes.[8] Their optimized structure shows bidentate binding of a single methyl sulfate to the cations.

Here, we apply DFT to study mixtures of ethyl sulfate and water binding to a single monovalent cation: Li^+, Na^+, or K^+. A main focus of this work is on the structures of the first solvation shell and cation binding to the sulfate group. We calculate the optimized structures as a function of the number of sulfate molecules and water molecules. While this work predominantly treats the gas phase, we expect the binding geometries to be dominant structures in aqueous environments, as they were in our prior studies on ions in aqueous solution.[9–11] We compare and contrast the complex structures of the ethyl sulfates to previously calculated structures of acetates, which contain the carboxylate group.[12] The difference in the number of oxygen (O) atoms between the two ligands results in interesting differences in optimal structures. The binding free energies for a variety of structures are calculated, not just the optimal structures. This broad assessment is particularly relevant for larger numbers of sulfates and/or waters, where multiple structures occur with similar free energies to the optimal structure. The binding free energy is sensitive to the environment, and thus calculations treating an aqueous environment are also included.

Explicit treatment of waters binding to ions in conjunction with other ligands is especially important for determining the structure and energetics of the first solvation shell of the cation, which typically is the dominant part of the chemically specific interactions.[13–19] We will see the role played by hydrogen bonding of water in these complexes, and particularly the role of the hydrogen bonding geometry, for selecting configurations. In the sulfates, the four O atoms yield many possible configurations that satisfy good hydrogen bonding geometries, which leads to multiple low-energy structures. Given that some of the four O atoms bind and some do not, polarization and charge transfer is important in determining the energetics of the optimal structures.[20,21]

In our previous DFT calculations of optimal structures for acetate binding in the presence of water to monovalent cations, we found that complexes with two acetates have the lowest free energy.[12] For 6 and fewer waters, the carboxylate binding to the cations is monodentate and occupies the first solvation shell. As water is added to the system, hydrogen bonding between waters and carboxylate O atoms further stabilizes monodentate structures. Those structures, which have strong electrostatic interactions that involve hydrogen bonds of varying strength, are significantly polarized, with ChelpG partial charges that vary substantially as the bonding geometry varies. We also found this polarization in Li^+ binding to sulfonate and sulfate ligands without water,[22] which agrees with related recent work.[23] For monodentate binding, the O atoms that do not bind to the cation have a different charge state, yielding significant polarization of the ligand.

The DFT methods used here are described in the Model and Methods section. In the Results section, we first present the binding free energy as a function of the number of ethyl sulfates and water molecules. Subsequently, we discuss the optimized structures for the complexes. Finally, we present the ChelpG charges and how the binding affects the charge distribution, implying the need for polarization in classical force fields. In the Discussion section, we compare the results for sulfates to that for carboxylates and address the specific characteristics of the sulfate binding. We end with our conclusions.

Model and Methods

The local cluster of n_S ethyl sulfate ligands about an ion I^+ in the presence of n_W waters corresponds to the following reaction,

$$\mathrm{I}^+ + n_\mathrm{S}\mathrm{CH_3CH_2SO_4^-} + n_\mathrm{W}\mathrm{H_2O} \rightleftarrows \mathrm{I}^+(\mathrm{CH_3CH_2SO_4^-})_{n_\mathrm{S}}(\mathrm{H_2O})_{n_\mathrm{W}}. \tag{1}$$

These gas phase calculations treat the clustering equilibria as taking place in an idealized environment that does not influence the reaction through long-ranged dispersive and electrostatic interactions or structural constraints on the clusters, except in terms of the number of sulfates and waters.[12,22,24–31] Our treatment is thus equivalent to an uncoupled quasi-chemical analysis carried out in a low dielectric environment (ϵ=1).[32–34] As a first approximation, this treatment is also appropriate for a nonaqueous system with low dielectric. For treatment of aqueous systems, we perform calculations using the polarizable continuum model (PCM).[35] In the supplemental information (SI), we provide calculations comparing the free energy of hydration for acetate to experimental data. No experimental data on sulfates is available for comparison.

We used the same methods as in recent calculations for acetate and water binding to monovalent cations.[12] We calculated the free energy change (ΔG) for the reactions in Eq. 1 using the Gaussian 16 quantum chemistry package and normal mode analysis of the vibrational states.[36,37] The free energy difference ΔG between the product (p) and the sum of the reactants is evaluated as follows

$$\Delta G = G_\mathrm{p} - (G_\mathrm{I} + n_\mathrm{S}G_\mathrm{S} + n_\mathrm{W}G_\mathrm{W}), \tag{2}$$

where G_X is the free energy of the individual molecule X, where subscripted I, S, and W represent ion, sulfate, and water.

The geometry optimizations were carried out in the gas phase using the density functional theory approach with the hybrid ωB97X-D approximation to the exchange-correlation energy.[38] This choice is based on previous work on DFT of ionic systems[12,39,40] and treats the van der Waals interactions, which are important for the large clusters treated here. For the basis sets, we used Dunning's correlation-consistent polarized double-zeta basis sets augmented with diffuse functions (aug-cc-pvDz).[41,42] All energies include the zero-point energy. Approximations include neglect of the basis set superposition error (BSSE), which is not included in the tables. For small clusters, the BSSE is small, no larger than 1 kcal/mol. The BSSE grows with cluster size (see SI for values for selected complexes). Nevertheless, BSSE is small relative to energy differences, which are of interest here. If absolute values were important, BSSE could be included. As described earlier,[16] free energies are calculated using a normal mode analysis that yields harmonic frequencies that are expected to represent the vibrational motions for small ion-ligand clusters.[37] A perturbative analysis of anharmonicity in the electronic energy surface for clusters of ions and waters confirmed that vibrations in small clusters with four (4) or fewer ligands are well-described by normal mode analysis.[43] For larger clusters, anharmonic effects are relevant and can be included easily in the final result. To treat anharmonic effects,[33,44,45] AIMD simulations of the liquid state are necessary, which is a treatment for a separate article.

Results

Free Energies

The gas phase free energy differences ΔG calculated from Eq. 2 are plotted in Figure 1 as a function of the number of ethyl sulfates n_{S} and number of water molecules n_{W} for a single cation, and no cation. We use the notation (n_{S}, n_{W}) to designate the number of ethyl sulfates and waters in a complex. For example, (2,3) denotes a complex with 2 ethyl sulfates and 3 waters. In addition, the plot includes the ΔG for a single ethyl sulfate binding to n_{W} waters but no cation. Those (open) points have the the highest, least favorable ΔG in each of the subplots. Tables 1 and 2 give the values except for the no sulfate cases, which were published previously.[22]

The dependence of ΔG on cation type, n_{S}, and n_{W} has some simplifying features (Figure 1) First, the ΔG follows the order $\mathrm{Li}^+ < \mathrm{Na}^+ < \mathrm{K}^+$, which corresponds to the smaller ion size having shorter bonds and thus stronger electrostatic binding, which dominates the free energy. The strongest binding occurs for n_{S}=2 for all cation types. For a fixed n_{W}, there is an approximate quadratic dependence on n_{S} (see solid lines in Figure 1). The figure also shows that (5, 0) structures are expected to have $\Delta G > 0$. Consequently, we limited our calculations to $n_{\mathrm{S}} = 4$. For a fixed n_{S}, ΔG decreases slightly to more favorable values with n_{W}. All these results follow trends found previously for the carboxylate ligand, acetate.[12]

The free energies of waters only binding to a single ethyl sulfate (1,n_{W}) are relatively high compared to the complexes with a cation. Table 2 shows that ΔG decreases in the ion-free cases from –4.1 kcal/mol to −10.8 kcal/mol as n_{W} goes from 1 to 6. At the large n_{W}, it appears that ΔG is saturating. We note, however, that anharmonic contributions to the free energy become relevant for large n_{W}, which are not considered here as they require a statistical evaluation involving ab initio molecular dynamics (AIMD).[26] These values are 1 to 2 orders of magnitude smaller (less favorable) than the strong ionic binding free energies for the sulfate with a cation (and water). In particular, substituting an ethyl sulfate for a water, that is, going from (0,n_{W}) to (1,n_{W}-1), results in a substantial drop in ΔG for all n_{W} and cation types. Almost all the other complexes with n_{S}=1 to 3 have ΔG that is more than 50 kcal/mol lower (more favorable) than the (0,n_{W}) values. The only exceptions are (4,0) and (4,1), where the repulsion of the net -3 charge yields ΔG above the (0,4) and (0,5) values.

The structural dynamics are related to the free energy barriers between complexes with one more or less molecule in the complex. The change in ΔG for adding or subtracting a water is small, a few kcal/mol, as can be see in Table 1. In particular, considering the lowest energy n_{S}=2 structures, the cost of moving a water molecule is low. In contrast,

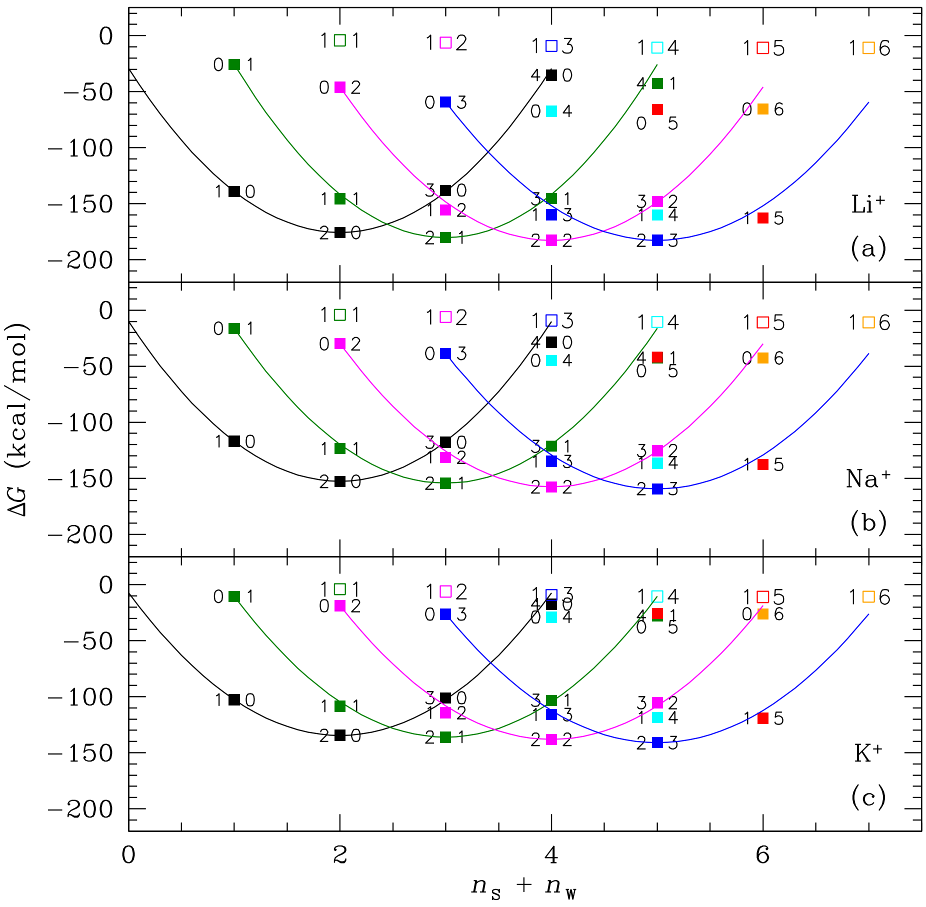

Figure 1: The free energy difference ΔG for varying numbers of sulfates n_{S} and waters n_{W} binding to (a) Li$^+$, (b) Na$^+$ and (c) K$^+$ The number of ions n_I is 1 for solid points and 0 for open points. The numbers by the points are n_{S} (left) and n_{W} (right). The data for fixed n_{W} are fit by a quadratic, shown as a solid line with varied color to distinguish the cases. The point color varies with n_{W}.

the cost of adding or subtracting an ethyl sulfate is large due to the quadratic dependence of ΔG on n_{S}. The other relevant pathway is along the vertical direction in Figure 1 or for constant $n_{\mathrm{S}} + n_{\mathrm{W}}$. In particular, considering the most optimal state (2,2) without second shell constituents, the next closest state is (1,3) The free energy differences between (2,2) and (1,3) are -22.8, -23.4 and -21.6 kcal/mol for Li$^+$, Na$^+$, and K$^+$, respectively. These differences are large enough that transitions are not likely to occur thermally and clusters with (2,2) structure are likely to be stable. This applies to the gas phase and to low dielectric media, where the barriers will be smaller, but still large compared to the thermal energy, $\mathrm{k_B}T$.

Most sulfate systems are aqueous and thus we have used PCM to calculate binding free energies in water. Table 3 has these ΔG_{W} for each cation for two values of n_{S}. The contrast to the gas phase is noteworthy, and not surprising given that these ionic systems dissolve in water. All the ΔG_{W} are small and positive, indicating the components are more stable than the complex, i.e. the complex dissolves. The magnitude decreases as Li$^+$ > Na$^+$ > K$^+$, which again corresponds with the stronger electrostatic binding of Li^+. The ΔG_{W} for K^+ is only 0.4 kcal/mol, which suggests that the complex is marginally unstable. We consider n_{S}=2 since two ethyl sulfates are the most stable for each cation in the gas phase. In the aqueous phase, the free energy increases enough that these are not likely structures.

Table 1: Binding free energies in kcal/mol for each cation with n_S ethyl sulfates and n_W waters.

n_{S}	n_{W}	$\Delta G(\mathrm{Li}^+)$	$\Delta G(\mathrm{Na}^+)$	$\Delta G(\mathrm{K}^+)$
1	0	-139.1	-117.1	-102.7
1	1	-145.6	-123.6	-108.4
1	2	-155.6	-131.4	-114.4
1	3	-159.8	-135.0	-116.0
1	4	-159.9	-136.1	-118.6
1	5	-162.6	-137.8	-119.0
2	0	-175.6	-152.6	-134.6
2	1	-180.2	-154.3	-136.1
2	2	-182.6	-157.6	-138.0
2	3	-182.7	-159.4	-140.9
3	0	-137.8	-117.9	-101.0
3	1	-145.3	-121.3	-103.2
3	2	-147.9	-125.3	-105.5
4	0	-35.0	-28.7	-17.4
4	1	-42.6	-39.9	-27.9

Table 2: Binding free energies in kcal/mol for single ethyl sulfate binding to n_{W} waters.

n_{W}	1	2	3	4	5	6
ΔG	-4.2	-6.1	-9.2	-10.5	-10.8	-10.9

Table 3: Binding free energies using PCM with water in kcal/mol for each cation and n_{S} ethyl sulfates.

n_{S}	$\Delta G_{\mathrm{W}}(\mathrm{Li}^+)$	$\Delta G_{\mathrm{W}}(\mathrm{Na}^+)$	$\Delta G_{\mathrm{W}}(\mathrm{K}^+)$
1	2.8	1.4	0.4
2	9.0	7.1	4.4

Structures

Sulfates have four O atoms: 3 terminal oxygens (labeled OS) and one nonterminal oxygen, which is the ether O that binds to a C atom (labeled OE). The ether O is an intrinsically different O type than the terminal O atoms, and we find binding to the ether O atom is preferred in some cases. In general, the optimal structures for complexes with water maximize the number of hydrogen bonds the water molecules can make. For sulfates, the additional O atoms compared to carboxylates, in particular, increases the possibilities for hydrogen bonding and yields some different geometries compared to the carboxylate group. With all the possible binding options, there are multiple configurations that have free energies within the accuracy of DFT calculations for the lowest free energy and all should be considered optimal, a problem also noted earlier for simpler anions.[46] In addition, there would be a distribution of these structures in a liquid, making them more broadly relevant. Given the large number of complexes, we focus the discussion on the calculated, optimal complexes for each (n_{S},n_{W}) pair that have the lowest calculated free energy. We discuss a few specific cases to describe aspects of the binding geometry that yield closely related free energies.

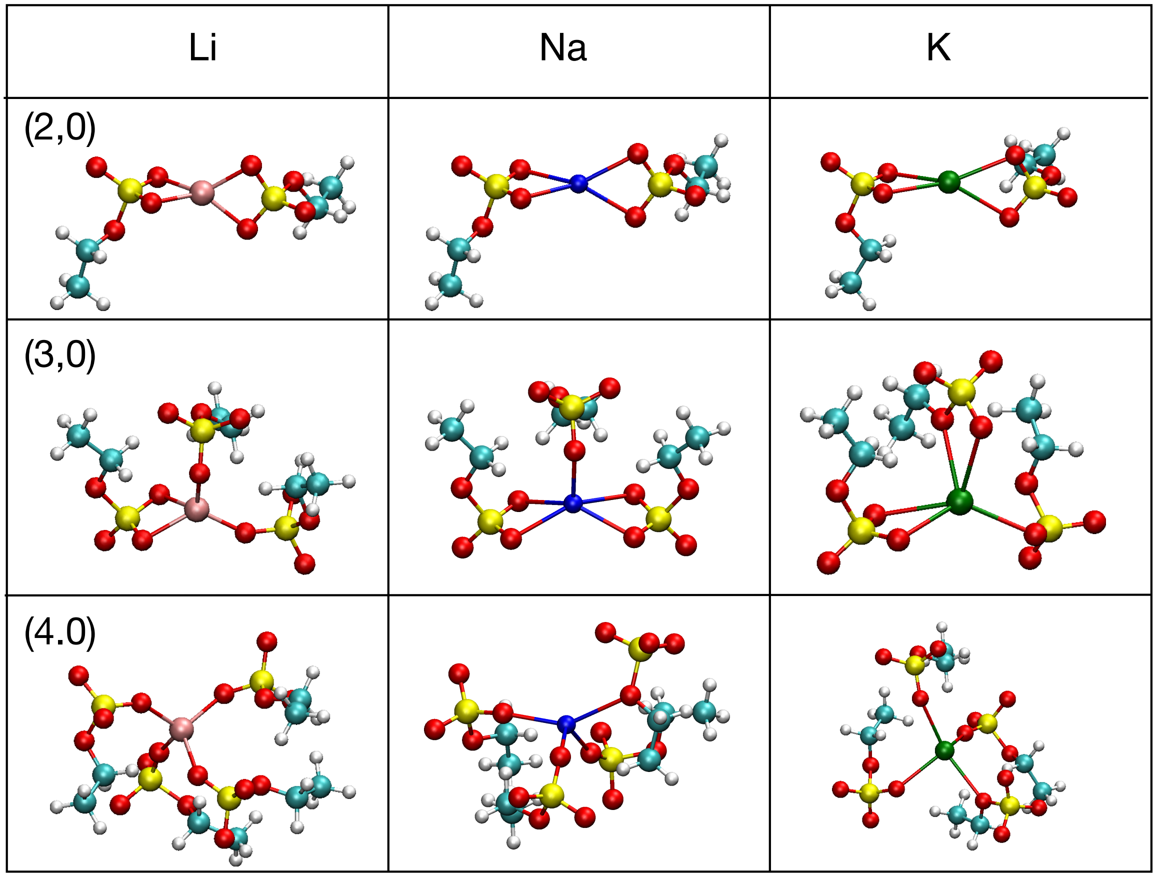

Figure 2: Images for the optimal structures for which n_S=2, 3 and 4 ethyl sulfates (and no waters) bind to the cations Li^+, Na^+ and K^+. The colors are white H, cyan C, yellow S, red O, pink Li, blue Na and green K.

More details of the many structures with a binding free energy within about a kcal/mol of the lowest is given in the SI.

We first consider the structures of complexes without water, which correspond to the (n_S, 0) solid points in Figure 1 that are connected by black lines. For a single ethyl sulfate and any one of the cations, the lowest free energy structure of all these complexes is bidentate binding of the cation to two of the terminal O atoms (OS) in the sulfate group. The overall lowest energy structure without waters is at n_S = 2 for all the cations and the cation is 4-fold coordinated by bidentate binding of both ligands (Figure 2). This 4-fold geometry of the coordinating O atoms resembles the carboxylate bidentate binding.[30]

A significant structural difference in comparison to carboxylates is the 4 and 5-fold structures for (3,0). None of the sulfate structures at (3,0) are 3-fold, as the optimal carboxylate binding is for all three cations. Figure 2 shows the optimal structures for each of the cations. The Li^+ structure is 4-fold coordinated, as expected with one bidentate and two monodentate sulfates. In contrast, both Na^+ and K^+ structures are 5-fold, with two bidentate and one monodentate bindings. For K^+, one of the bidentate structures involves the ether O atom. A structure that has a terminal O instead is only 0.4 kcal/mol higher. Thus, there is little difference in which O atom forms the bidentate structure in this case, and both would exist thermally. Since Na^+ and K^+ can prefer coordinations with O atoms larger than 4, the 5-fold coordination is consistent and the sulfate O geometry enables this coordination geometry.[10]

When n_S increases to 4, the binding becomes monodentate for each of the sulfate ligands and achieves a 4-fold coordination, as shown in Figure 2 for all the cations. For the K^+ case, one of the binding O is an OE. Attempts to optimize with an OS instead results in convergence to the OE binding. Overall, in the (n_S, 0) structures with just sulfate ligand binding to a cation, 4-fold coordination of the cation occurs most often. The exceptions occur at n_S=3, where the Na^+ and K^+ structures are 5-fold coordinated by two bidentate sulfates and one monodentate. At n_S=4, the monodentate structures are favored, presumbaly because this geometry more uniformly spreads the negative charge of the sulfates.

The structures with the lowest ΔG in Figure 1 are the (2,n_W) complexes. Their lowest free energy structures are shown in Figure 3. Among those structures, there is significant variety as a function of cation type and n_W. All the Li^+ complexes are 4-fold coordinated, which is typical for Li^+ and different ligands.[22,30,47–50] In contrast, the coordination n_c for Na^+ is only 4 for n_W=1, and 5 for larger n_W. For K^+, $n_\mathrm{c} = 5$ for all n_W. Bidentate binding is part of the 5-fold coordination for K^+ at each n_W, including bidentate with the ether O. At n_W=1, all cations have bidentate binding as it is necessary to obtain at least $n_\mathrm{c} = 4$. At n_W=3, one of the waters is in the second shell for K^+ and Li^+. For Na^+, however, both sulfates are monodentate and all waters bind to Na^+. Nevertheless, a structure with a bidentate sulfate and water in the second shell is only 0.1 kcal/mol higher for Na^+. This is another example of the multiple structures that are indistinguishable within the accuracy of DFT. Even within the lowest free energy structures found, there is much variety in the structures at (2,n_W). This result highlights that there will be multiple distinct structures involving the sulfate ligand, especially when considered in a condensed state.

At n_W=1, the additional O atoms in the sulfate group enable $n_\mathrm{c} = 4$ for Li^+, which contrasts with the $n_\mathrm{c} = 3$ binding of the carboxylate.[12] Figure 3 shows that, as in the carboxylate geometry, the shorter O:Li^+ bonds enable the water molecule to form hydrogen bonds to both sulfates. Whereas in the carboxylate this hydrogen bonding occupies all the O atoms, the sulfate, with its additional O atoms, can have bidentate binding to achieve $n_\mathrm{c} = 4$. Also, similar to the carboxylate geometry for Na^+ and K^+, this double hydrogen bonding is not possible in these alkali metals because of their larger cation bonds to O. Consequently, the water can only bind to one sulfate for these cations. The coordination then depends on whether both sulfates bind in bidentate form or not. For Na^+, the lowest free energy structure has one mondentate sulfate and $n_\mathrm{c} = 4$. There is a 5-fold structure for Na^+ with two bidentate sulfates that is only 0.2 kcal/mol higher. In the lowest energy structure for K^+, the sulfates bind in bidentate mode and, along with the water binding to the K^+, yield a 5-fold coordination. While a 4-fold structure exists for K^+, the ΔG is 2.6 kcal/mol higher. Even for the relatively simple case of two sulfates and one water, there are distinct optimal structures as a function of cation, and there are multiple structures with small free energy differences. This complexity occurs because the sulfate geometry enables multiple, similar binding geometries that consequently have similar free energies.

For the (2,2) structures, significant variation occurs among the cation type. The Li^+ structure is 4-fold coordinated, but the Na^+ and K^+ are 5-fold coordinated. The waters are in the first shell for all the cations at this n_W. For Li^+, the ethyl sulfates have monodentate binding. The Na^+ and K^+ lowest energy structures are topologically

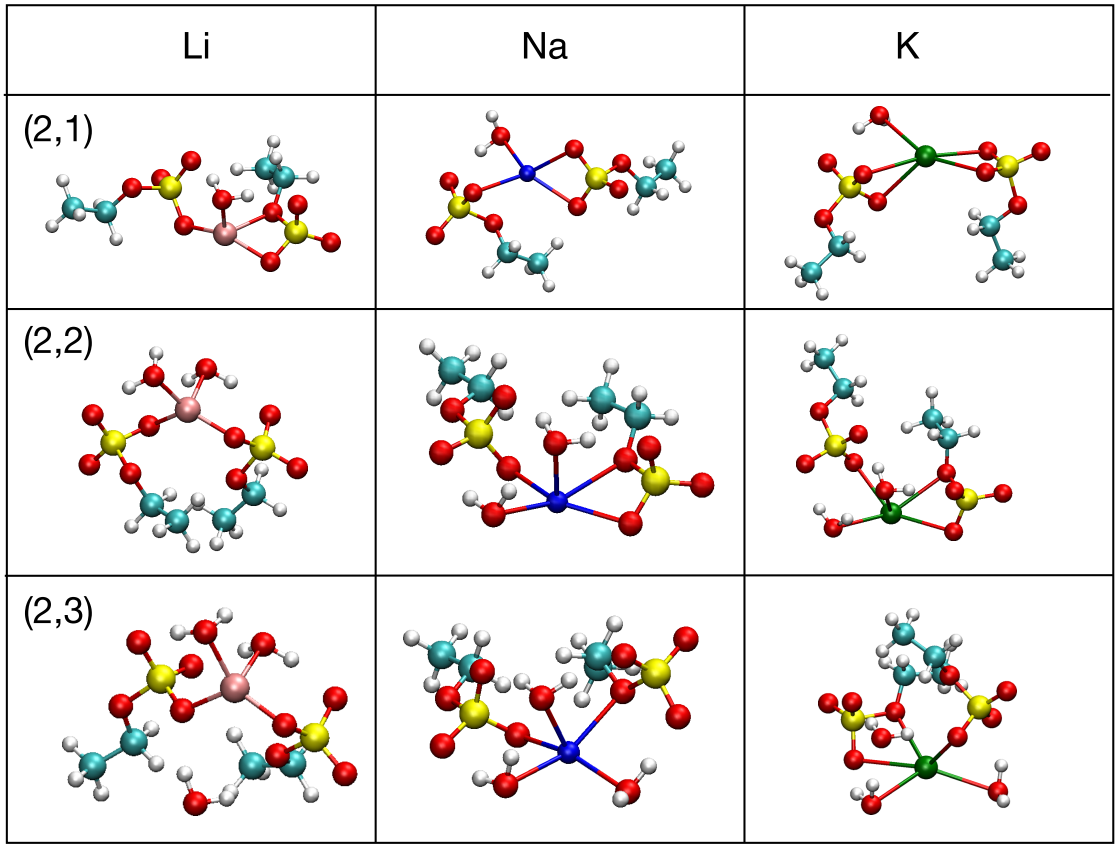

Figure 3: Images[51] of lowest free energy structures at $(n_{\mathrm{S}}, n_{\mathrm{W}})$ for $n_{\mathrm{W}} = 1 - 3$ for Li^{+}, $\mathrm{Na}^{+}$and K^{+} at $n_{\mathrm{S}} = 2$.

the same, with one bidentate and one monodentate sulfate binding. For Na^+, a 4-fold structure with both sulfates in monodentate mode has ΔG just 0.4 kcal/mol higher. No 4-fold structure with comparable free energy was found for K^+.

For the (2,3) structures, the addition of the third water goes to the second shell for Li^+ and for K^+, but not Na^+. The binding to Li^+ has a 4-fold coordination similar to the (2,2) structure, and the third water in the second shell hydrogen bonds to both sulfate groups. The K^+ structure is 5-fold coordinated, with one sulfate being monodentate. The other sulfate is bidentate, with the ether O binding. Two of the waters bind to K^+ to make the 5-fold coordination and the third water hydrogen bonds to the sulfate O not binding to K^+. The ether O is preferred in the bidentate binding, by 1.9 kcal/mol, because the ether binding geometry favors better hydrogen bonding by the waters. The Na^+ structure is 5-fold coordinated, but with all 3 waters binding and the sulfates have monodentate binding with one binding through the ether O. A structure similar to the K^+ structure with a water in the second shell is just 0.1 kcal/mol higher. This small difference shows that the sum of competing contributions to the free energy (e.g. oxygen:cation electrostatic binding, water hydrogen bonding, distribution of the O negative charges) can produce different geometries that result in close values.

The ΔG of the (3,1) structures (cf. Figures S5 and S7) for Na^+ and K^+ show there is a small trade-off between $n_c = 4$ and 5 for these cations. Both Na^+ and K^+ have the lowest energy structure with $n_c = 4$ and the sulfates are monodentate and the water binds to Na^+. However, an $n_c = 5$ structure exists for both. For K^+, one sulfate is bidentate, upping n_c to 5 with the free energy just 0.3 kcal/mol higher. For Na^+, the equivalent structure is 1.1 kcal/mol higher, and there is another $n_c = 5$ structure with two bidentate sulfates and the water in the second shell that is 0.9 kcal/mol higher. Another interesting difference is the $n_c = 4$ structure with one of the monodentate sulfates using the ether O to bind, which has a free energy 1.0 kcal/mol higher than the optimal structure and all the monodentate O atoms as terminal O. For Li^+, a bidentate sulfate is expensive, at 4.3 kcal/mol higher in free energy, because Li^+ structures are $n_c = 4$ and the bidentate geometry pushes the water to the second solvation shell.

In SI Figures S7-S9, multiple converged configurations for each cation in the (2,1) complexes are shown and, in the corresponding Tables S4-S6, the free energies and bonding characteristics are given. For Li^+, the (2,0) structure without water has both sulfates binding in bidentate mode to the Li^+, and there are no other structures that have similar ΔG. Adding a water to obtain (2,1) changes the binding significantly. A structure with the water in the second shell hydrogen bonding to each of the bidentate binding sulfates has ΔG almost 5 kcal/mol higher than the lowest energy structure. The group of low free energy structures all have the water binding directly to the Li^+. Interestingly, the lowest free energy structure (Figure S7F) has one bidentate sulfate with the ether O. Calculations starting with a bidentate structure using only terminal O converge to structures with the ether O. Surprisingly, there is a 3-fold structure that is within 0.4 kcal/mol of the lowest free energy structure. This structure has both sulfates binding in a monodentate mode, and the water, besides binding to the Li^+, forms hydrogen bonds to both sulfates. Clearly, water binding to Li^+ that also hydrogen bonds to some O has lower free energy than only bidentate binding.

The structure at (2,1) for Na^+ and K^+ differ from Li^+ because the former two can be 5-fold coordinated. For Na^+ at (2,1), the lowest free energy structures have water binding directly. Nevertheless, one structure with a second shell water (Figure S8A) has ΔG just 0.7 kcal/mol higher. This optimal structure is 4-fold coordinated by one sulfate in bidentate mode and the other monodentate. However, an $n_{\mathrm{c}} = 5$ structure exists that is only 0.2 kcal/mol higher. For K^+, the group of low free energy structures are 5-fold coordinated by both sulfates in bidentate mode and the water binding directly. In the lowest energy structure, the bidentate binding occurs only with the terminal O atoms and with an ether O in one ligand binding in bidentate mode. In that case, the free energy is just 0.6 kcal/mol higher. Interestingly, a tridentate state converged with ΔG 1.3 kcal/mol higher than lowest state. This is the only tridentate state we found.

For these cases with many low-lying structures, the ordering in terms of ΔG does not correspond to the order with respect to ΔH, which implies that entropy for these complexes plays a role, too. This is not surprising given, for example, that monodentate vs. bidentate binding yield different vibrational modes and if the enthalpy of the configurations are similar, then the entropy will determine the lower free energy. Detailed numerical comparisons are given in the SI.

Atomic Charges

We have previously addressed the charges on O atoms in the sulfate and sulfonate groups binding to Li^+.[22] One main point was that the ChelpG charge[52] on the O atom(s) binding to the Li^+ are different from the nonbinding O atoms. This differing charge distribution is to be expected given that not all the O atoms bind, yet is an important limitation for fixed charged force fields. We will show that this point applies to the sulfate group binding to other ions as well. In addition, the ether O atom can bind and its charge depends on the binding status.

The scaling of ion charge in fixed charge force fields has become common as this improves some results and has justification as a simple form of polarization.[53] In particular, for some electrolyte systems, charge scaling of ions has been successful in improving the agreement between simulation and experiment.[54] However, there are cases where charge scaling for electrolytes has been insufficient and explicit charge transfer has been required.[20,55–59] These simulations show that charge transfer is necessary because the combined role of the cation and anion in simple salts yields a structure-dependent charge scaling that differs for cations and anions.[21]

Since the cation is free in our motivational systems while the anion is typically bound to a macromolecule, we are more focused on the environment about the cation. In addition, we are particularly interested in cases where the cation directly interacts with the anion, as in ion channels. This environment will produce different results than ions in an aqueous environment,[60] where both anions and cations are free to diffuse and water tends to solvate the ions distinctly. Thus, situations where charge transfer has been important are not likely or as prominent. In any case, the present DFT calculations provide important information about the interactions, structure and charge distributions for these systems. The results show that polarization beyond simple charge scaling will be necessary for highly accurate force fields.

Charge variation is apparent in Figure 4, which shows the ChelpG charges for the optimized structure at (2,2) for Na^+. In this structure, Na^+ is 5-fold coordinated by both waters binding and bidentate binding by the ethyl sulfate on the left along with the OE atom on the right with charge -0.544 binding. The ethyl sulfate on the right has monodentate binding. The charges on the terminal sulfate O atoms are distinct, and there is a significant difference in the ether oxygen atom charge because one binds and one does not. The water O atoms have the most negative charge of all the O atoms because of the polarizability of water and the negative charge of the sulfate ligand being shared among multiple O atoms, which reduces the charge on individual atoms.

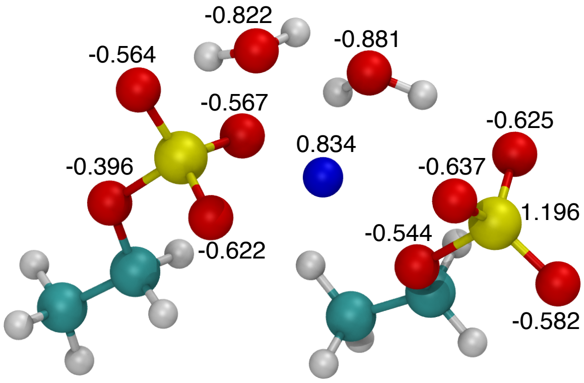

Figure 4: The ChelpG charges for the optimized structure of Na^+ at (2,2).

Below we first discuss the average charges over all the systems for each cation to characterize how the charge is distributed. In particular, we address how the -1 charge is distributed in the sulfate ligands. The detailed ChelpG charges for O atoms in the optimal structures are given in Tables S3-S8 for all the cations. After the discussion of the average distribution, we examine the charges for specific complexes and address how the charge distribution varies due to the structure of the complex.

The averages of the ion charges over all systems in units of electron charge are 0.78(4), 0.82(7) and 0.80(8) for Li^+, $Na^+$and K^+, respectively. Interestingly, the values are near 0.80, which is a common value used in fixed charged MD simulations, particularly when scaling the charges to treat the first order effect of polarization.[61] However, while this scaled charge may improve the simulations, it does not address the charge variation in the O atoms binding to the cations, which we discuss below. The average charge on the S atom is 1.13(15), 1.07(17), and 1.11(13), for the Li^+, Na^+ and K^+ systems, respectively. The average S charge is above +1 for all the cations, indicating some negative charge has been donated from the S to the bonded O atoms.

To address the distribution of the -1 net charge on the sulfate ligand, we calculated the sum of the charges on the terminal OS atoms and the S atom as a group. In the base picture of the sulfate group, a charge of -1 should be dispersed among the terminal OS atoms (with possibly some going to the OE atom). Again, we consider the average dispersal of the charge over all the complexes. The standard deviations for the charge sums are small, indicating that, while the individual atomic charges can have larger variation, their sums are more constrained. The average net charge of the SO_3 group is -0.70(3), -0.70(5) and -0.69(5), for Li^+, Na^+, and K^+ systems, respectively, which is close to the average cation charge of about +0.8. Thus, a single SO_3 group would neutralize a cation mostly, which implies the charge on the ligand could remain primarily in the terminal atoms for complexes with low net charge. However, since the ether O atoms bind in some cases, we also calculated the charge sum including this fourth O atom, finding the average to be -1.15(9), -1.14(11), and -1.14(11) for Li^+, $\mathrm{Na}^+$and K^+ systems, respectively. These values are remarkably similar among the cation systems. This sum shifts the total charge to the ligand headgroup by about -0.4, which, as we show below, matches the average charge on the OE atom. In order to conserve the total charge, some positive charge must occur elsewhere in the ligand. The C atom binding to the OE is mostly responsible for bringing the net charge of the sulfate molecule to -1.0.

The average charges, obtained by summing over the optimal systems on the terminal sulfate O atoms (OS), the sulfate ether O atoms (OE) and the water O atoms (OW), are given in Table 4. The average values show clear differences among the three types of O atoms. The OS atoms have a larger charge than the OE atoms, which is to be expected. The water O atom charges are larger than the OS charges. The single charge being shared among 3 OS atoms will constrain the charge values for OS. While water is not charged, the large OW charge is indicative of water's strong polarization. We note that the common 3-point water models[62,63] have OW charges of about -0.83, which are close to the values in Table 4. This agreement suggests that, on average, the fixed charged models will be sufficiently accurate. Simulations of behavior that depends on the specific binding of individual O atoms and cations will be the ones where fixed charges will fail.

Table 4: Average charge ,$\langle q \rangle$, and standard deviation, σ_q, of ChelpG charges for the sulfate terminal O atoms (OS), ether O atoms (OE), and for the water O atoms (OW).

cation	$\langle q_{\mathrm{OS}} \rangle$	σ_q	$\langle q_{\mathrm{OE}} \rangle$	σ_q	$\langle q_{\mathrm{OW}} \rangle$	σ_q
Li	-0.613	0.058	-0.449	0.096	-0.804	0.049
Na	-0.592	0.071	-0.438	0.090	-0.820	0.056
K	-0.601	0.060	-0.443	0.095	-0.819	0.067

The charge of the O atoms vary significantly beyond the average values. We first consider the ChelpG charges on sulfate O atoms (OS and OE) for systems without water, given in Table 5. This data shows the differences in the charges between the binding (B) and nonbinding (NB) O atoms. For bidentate binding by two terminal O atoms that occurs for smaller n_{S}, the binding OS charge is larger than the third nonbinding terminal O atoms. For larger n_{S}, for which the complex has a net negative charge and monodentate binding, the binding terminal O atom typically has *lower* charge than the other terminal O atoms. Because of the net negative charge, more charge is on the nonbinding O that are more spread out, reducing the electrostatic repulsion between them and lowering their energetic cost. In general, the ether O atom has a lower charge than the terminal O atoms (OS) even when the OE binds to the cation. The greatest variation is seen in the ether O depending on whether it binds or not. For coordination greater than 4, the ether O often participates in the binding to Na^+ and K^+, but not Li^+ which is 4-fold coordinated.

The n_{S}=2 structure has the lowest free energy for each of the cation systems, and the structures are particularly symmetric (cf. Fig. 2) especially compared to larger n_{S} structures. Consequently, the charge distribution has little dependence on the cation in the complex. For n_{S}=3 and 4, the coordinationvaries with cations and, consequently, the charges on O atoms vary accordingly.

When the ether oxygen participates directly in binding to the cation, the charge distribution is significantly affected for that sulfate molecule. This effect is clearly noticeable at (3,0) for the K^+ complex, which is 5-fold coordinated with an ether O participating in a bidentate bond, yielding distinct charge values. The OE charge in the bidentate case is much lower (-0.183) than the other cases, and the corresponding binding OS atoms have the lowest charge of the binding OS atoms at (3,0). While the optimal structure at (3,0) for Na^+ is also 5-fold, none of the OE bind to Na^+. The charge variation is consequently small. In the (4,0) complexes, all the binding is monodentate, but the lowest energy structure for the Na^+ and K^+ complexes have an OE making one of the monodentate bindings. The charge on this OE is again much smaller than other nonbinding OE. For K^+, $q_{\mathrm{OE}} = 0.247$ and for Na^+, $q_{\mathrm{OE}} = 0.289$ while the nonbinding OE for both cations have charges > 0.50. Thus, the OE bidentate binding significantly alters the charge distribution in the complex.

Table 5: ChelpG charges in units of e for the three O atoms in the sulfate group of the optimized structures without waters as a function of the number n_{S} of ethyl sulfate ligands.

ion	n_{S}	q_1 [a]		q_2		q_3		q_{OE}	
Li^+	1	-0.670	B	-0.627	B	-0.455	NB	-0.378	NB
Na^+	1	-0.683	B	-0.642	B	-0.487	NB	-0.395	NB
K^+	1	-0.607	B	-0.642	B	-0.508	NB	-0.413	NB
Li^+	2	-0.623	B	-0.602	B	-0.560	NB	-0.427	NB
Li^+	2	-0.627	B	-0.600	B	-0.561	NB	-0.433	NB
Na^+	2	-0.627	B	-0.607	B	-0.565	NB	-0.437	NB
Na^+	2	-0.630	B	-0.606	B	-0.565	NB	-0.438	NB
K^+	2	-0.627	B	-0.607	B	-0.565	NB	-0.437	NB
K^+	2	-0.630	B	-0.606	B	-0.565	NB	-0.438	NB
Li^+	3	-0.610	B	-0.623	NB	-0.602	NB	-0.523	NB
Li^+	3	-0.690	B	-0.657	NB	-0.634	NB	-0.562	NB
Li^+	3	-0.674	B	-0.657	B	-0.611	NB	-0.534	NB
Na^+	3	-0.609	B	-0.622	NB	-0.611	NB	-0.495	NB
Na^+	3	-0.648	B	-0.653	B	-0.609	NB	-0.534	NB
Na^+	3	-0.682	B	-0.660	B	-0.615	NB	-0.534	NB
K^+	3	-0.660	B	-0.632	NB	-0.637	NB	-0.504	NB
K^+	3	-0.653	B	-0.664	B	-0.617	NB	-0.538	NB
K^+	3	-0.597	B	-0.647	NB	-0.611	NB	-0.183	B
Li^+	4	-0.664	B	-0.677	NB	-0.681	NB	-0.391	NB
Li^+	4	-0.620	B	-0.701	NB	-0.677	NB	-0.570	NB
Li^+	4	-0.622	B	-0.667	NB	-0.659	NB	-0.502	NB
Li^+	4	-0.615	B	-0.717	NB	-0.684	NB	-0.562	NB
Na^+	4	-0.600	B	-0.663	NB	-0.644	NB	-0.536	NB
Na^+	4	-0.627	B	-0.645	NB	-0.642	NB	-0.551	NB
Na^+	4	-0.654	B	-0.660	NB	-0.681	NB	-0.538	NB
Na^+	4	-0.616	NB	-0.657	NB	-0.653	NB	-0.289	B
K^+	4	-0.578	B	-0.665	NB	-0.649	NB	-0.519	NB
K^+	4	-0.593	B	-0.645	NB	-0.639	NB	-0.554	NB
K^+	4	-0.630	B	-0.658	NB	-0.679	NB	-0.503	NB
K^+	4	-0.602	NB	-0.649	NB	-0.649	NB	-0.247	B

[a] B represents binding to Na^+ and NB is nonbinding

For the complexes with no waters, the sum of the charge on the sulfate and the cation equals the next charge, that is, $-N_S + 1$. The charge on the cation is always less than +1; thus, some charge is transferred to the cation. Overall, this situation corresponds to charge redistribution within molecules and overall charge scaling. This effect can be handled by a charge-scaled, polarizable force field.

The ChelpG charges for the n_{S}=2 complexes with n_{W}=1-3 (cf. Figure 3) are given in Table 6 for all the cations. The OS atom furthest from the cation (3rd OS in table) almost always has the lowest charge of all the OS atoms. The closest and binding OS atom typically has the most negative charge in its sulfate group. The OE charge is almost always the lowest charge of the O atoms, even when it binds to the cation. Overall, with water in the complexes, the charge of the OE binding to the cation is larger than other nonbinding OE, which contrasts to the behavior without water.

The charge state of the OW varies as a function of n_{W}, and does not have an overall singular behavior, because the binding geometry varies as a function of (n_{S},n_{W}) and cation type. We briefly describe the water oxygen charge as a function of n_{W} for n_{S}=2. For n_{W}=1, the OW charge is ordered by cation size, with the Li^+ complex having the most negative. In contrast to Na^+ and K^+, the bidentate binding for the Li^+ includes the OE atom, and its charge is larger than the other OE charge and least charged OS atom. For n_{W}=2, the OW charges are no longer ordered by the cation size. Both Na^+ and K^+ achieve 5-fold coordination by involving a bidentate sulfate with the OE atom participating. In these cases, the charge on the OE binding atom is more negative than for the nonbinding OE in the other sulfate, providing a stronger electrostatic interaction. At n_{W}=3, Na^+ is rather distinct in having one monodentate sulfate binding through the OE atom and having all 3 OW atoms bind, whereas Li^+ and K^+ only have two OW atoms bind. The charges on the two binding OW are similar across the cations, but the nonbinding OW are different for Li^+ and K^+.

Table 6: For n_{S}=2 complexes with n_{W}=1-3, the ChelpG charges of sulfate O atoms binding in units of electron charge.

ion	n_{W}	OS[a]	[b]	OS		OS		OE		OW		OW		OW	
Li^+	1	-0.657	B	-0.640	NB	-0.571	NB	-0.575	B	-0.888	B				
Li^+	1	-0.666	B	-0.577	NB	-0.561	NB	-0.428	NB						
Na^+	1	-0.620	B	-0.601	B	-0.563	NB	-0.452	NB	-0.792	B				
Na^+	1	-0.652	B	-0.598	NB	-0.564	NB	-0.435	NB						
K^+	1	-0.626	B	-0.630	B	-0.571	NB	-0.457	NB	-0.760	B				
K^+	1	-0.623	B	-0.579	B	-0.572	NB	-0.404	NB						
Li^+	2	-0.650	B	-0.613	NB	-0.574	NB	-0.444	NB	-0.788	B	-0.794	B		
Li^+	2	-0.605	B	-0.602	NB	-0.562	NB	-0.385	NB						
Na^+	2	-0.637	B	-0.625	NB	-0.582	NB	-0.544	B	-0.822	B	-0.881	B		
Na^+	2	-0.622	B	-0.567	NB	-0.564	NB	-0.396	NB						
K^+	2	-0.633	B	-0.655	NB	-0.584	NB	-0.529	B	-0.819	B	-0.900	B		
K^+	2	-0.586	B	-0.546	NB	-0.555	NB	-0.398	NB						
Li^+	3	-0.653	B	-0.616	NB	-0.566	NB	-0.534	NB	-0.869	B	-0.793	B	-0.818	NB
Li^+	3	-0.668	B	-0.580	NB	-0.581	NB	-0.412	NB						
Na^+	3	-0.615	B	-0.555	NB	-0.548	NB	-0.391	NB	-0.866	B	-0.816	B	-0.798	B
Na^+	3	-0.607	NB	-0.636	NB	-0.564	NB	-0.500	B						
K^+	3	-0.654	B	-0.594	NB	-0.560	NB	-0.401	NB	-0.850	B	-0.808	B	-0.862	NB
K^+	3	-0.623	B	-0.621	NB	-0.562	NB	-0.548	B						

[a] Oxygen atom labels are OS for the terminal O atom, OE for the ether O atom and OW for the water O atom.
[b] B represents binding to Na^+ and NB is nonbinding.

For these systems with water, a net negative charge is transferred to the water molecules. The magnitude varies from -0.03 to -0.08. This magnitude is small enough that a force field with polarization (and without charge transfer) will have sufficient accuracy.

We have discussed the charges for only the lowest ΔG cases, in part for practical considerations. The basic points described above remain true for the wider variety of cases with free energies close to the optimal value. The OE has lower charge than the OS atoms. Binding O atoms have different charges than nonbinding, particularly within the same ligand.

Discussion

The (2,2) structures with 2 ethyl sulfates and 2 waters binding to a cation possess the main structural factors of the more general complexes. These factors include the coordination dependence on cation, monodentate vs bidentate binding, and water vs sulfate ligand binding, and they combine dependently to yield the optimal complex structure. The roles of the factors can be seen readily in the structures of the complexes with Li^+, which are the simplest since the optimal structures are almost always 4-fold. At (2,2), the Li^+ optimal structure has 2 monodentate sulfates and 2 waters binding to Li^+ to make the 4-fold structure. As waters are added to the (2,0) system, the waters preferentially bind to the Li^+, successively shifting the sulfate binding to be monodentate to achieve $n_\mathrm{c} = 4$. Adding an additional water (such as (2,3)) does not change n_c for Li^+. Instead, the water goes to the second solvation shell. Thus, (2,2) is at the boundary for second shell waters. For all the systems, the water O have a larger charge than the OS or OE atoms, making the electrostatic binding prefer the OW.

For Na^+ and K^+, the larger 5-fold optimal structures allow bidentate binding of one sulfate. The larger ion size of Na^+ and K^+ yields longer and, thus, weaker ionic bonds to the O atoms. Consequently, there are more binding geometries with similar binding free energies. For example, Na^+ has ΔG = -157.6 kcal/mol with a bidentate binding, but, at only 0.4 kcal/mol higher in free energy, there is a monodentate $n_\mathrm{c} = 4$ structure. In a similar vein, K^+ has a lowest energy $n_\mathrm{c} = 5$ structure with single bidentate binding at ΔG = -138.0 kcal/mol and, again, at only 0.4 kcal/mol higher there is another $n_\mathrm{c} = 5$ structure with both bidentate sulfate and one water in the second ion solvation shell. In general for $n_\mathrm{S} + n_\mathrm{W} \geq 4$, there is typically not a dominant lowest energy complex structure for Na^+ and K^+. Instead, there are multiple binding geometries that satisfy the conditions for coordination, hydrogen bonding, sulfate binding geometry and other properties that have binding free energies with 1-2 kcal/mol.

Comparing the sulfate complexes to those formed with the carboxylate ligand, acetate,[12] shows the role of the two ligand geometries in the binding of monovalent cations, including with waters. The carboxylate group, sharing an electron between two oxygen atoms instead of 3 for the sulfate, has a stronger electrostatic interaction and thus stronger binding free energies for the alkali metal ions. However, we note that recent work for more complex cations (e.g., guanidinium, methyl ammonium) found the opposite result, albeit with classical force fields.[23] Those larger cations have additional geometric and interaction constraints in forming the complex structure. For the atomic cations, the sulfate ligand, having 4 bondable O atoms (including the OE), has more binding geometries than the carboxylate. Consequently, there are more structures with free energies near the lowest free energy value. In addition, there are more bidentate geometries that are feasible geometrically as well as energetically. One clear example of different binding structures occurs in the (3,0) complexes. In acetate, the binding is monodentate for all 3 cations and 3-fold, but with the ethyl sulfate, at least one bidentate binding mode occurs and n_c = 4 or 5. With respect to waters, the more O atoms in a sulfate than in a carboxylate enable a larger number of geometries that maximize the number of hydrogen bonds per water molecule. This aspect also increases the number of low-lying free energy structures.

A more accurate functional or quantum chemistry method and basis set may find some variation in the lowest energy structures found with the ωB97X-D function and the aug-cc-pVdz basis given the number of structures that are within the uncertainty of the chosen functional and basis set. We have tried to make it clear that a small population of states is often relevant once the number of molecules in the complex reaches 4. In order to keep the presentation of the results to a reasonable length, we have focused on the calculated lowest energy structure, as determined by the present level of theory, and the next nearest case to give a sense of the competing interactions and geometries. We expect more accurate calculations will find a similar level of competition and energy population of structures.

Conclusions

Understanding the binding of the sulfate group to cations in the presence of water is important for a wide range of molecular systems. Calculations that treat the polarization and charge transfer are necessary for the strong electrostatic interactions involved in these complexes. To obtain sufficiently accurate results, we performed DFT calculations to identify the optimal structures and binding free energies for complexes of n_{S} ethyl sulfates and n_{W} waters binding to monovalent cations, Li^+, Na^+, and K^+. The gas phase binding free energies follow the order Li $<$ Na $<$ K, which corresponds to the smaller cation with shorter bonds having stronger electrostatic interactions and, thus, the lower, more favorable binding free energy. The same order was found for the carboxylate ligand.[12] The optimal structure without water shows 4-fold coordination by bidentate sulfates for each of the cations. The Li^+ structures remain predominantly 4-fold in the presence of waters, in part because Li ion's shorter bond length inhibits larger coordination. The coordination of the Na^+ and K^+ ions with waters tends to be 5, but there is variation among the different complex compositions of n_{S} and n_{W}. We find that water appears in the second shell of optimized structures, once a third water is included in the complex.

The sulfate ligand group with 4 binding O atoms can adopt many possible binding geometries, particularly for complexes with multiple sulfates and waters. The ester O in the sulfate sometimes preferentially binds to the cation over the other sulfate O atoms. This geometric variety yields a number of structures with similar, low-lying binding free energies. Particularly in comparison to the carboxylate ligand, the sulfate ligand has a wider range of binding geometries. The binding free energies are higher and less favorable than carboxylates due to the electron charge being dispersed among more O atoms.

We calculated the ChelpG charges to quantify the importance of polarization and charge transfer in the binding of the sulfate ligand to monovalent cations. The binding O typically contains more charge than non-binding and there always are non-binding O in the sulfate group. The ester O atom almost always has a lower charge than the terminal sulfate oxygens. When the ester O atom binds, its charge may be larger or smaller than other ester O atoms in the complex. Overall, the charge on the sulfate O atoms is not the same, which comprises a failure for fixed-charge force fields. This error may affect the coordination of cations and the distribution of bidentate vs. monodentate binding in those force fields.

Acknowledgements

This work was performed, in part, at the Center for Integrated Nanotechnologies, an Office of Science User Facility operated for the U.S. Department of Energy (DOE) Office of Science. Sandia National Laboratories is a multimission laboratory managed and operated by National Technology & Engineering Solutions of Sandia, LLC, a wholly owned subsidiary of Honeywell International, Inc., for the U.S. DOE's National Nuclear Security Administration under contract DE-NA-0003525. We gratefully thank Sandia's Laboratory-Directed Research and Development program for funding. The views expressed in the article do not necessarily represent the views of the U.S. DOE or the United States Government.

Supporting Information

Coordinate files, hydration free energies, MP2 calculations, images of optimized geometries and other low-lying structures, tables of ChelpG charges.

References

(1) Missel, P. J.; Mazer, N.; Benedek, G.; Young, C.; Carey, M. C. Thermodynamic analysis of the growth of sodium dodecyl sulfate micelles. *J. Phys. Chem.* **1980**, *84*, 1044–1057.

(2) Barbeyron, T.; Brillet-Guéguen, L.; Carré, W.; Carrière, C.; Caron, C.; Czjzek, M.; Hoebeke, M.; Michel, G. Matching the Diversity of Sulfated Biomolecules: Creation of a Classification Database for Sulfatases Reflecting Their Substrate Specificity. *PLOS ONE* **2016**, *11*, 1–33.

(3) Wolfenden, R.; Yuan, Y. Monoalkyl sulfates as alkylating agents in water, alkylsulfatase rate enhancements, and the "energy-rich" nature of sulfate half-esters. *Proc. Natl. Acad. Sci. U.S.A.* **2007**, *104*, 83–86.

(4) Funderburgh, J. L. Keratan Sulfate Biosynthesis. *IUBMB Life* **2002**, *54*, 187–194.

(5) Soares da Costa, D.; Reis, R. L.; Pashkuleva, I. Sulfation of Glycosaminoglycans and Its Implications in Human Health and Disorders. *Annu. Rev. Biomed. Eng.* **2017**, *19*, 1–26.

(6) Whitfield, D. M.; Tang, T. H. Binding properties of carbohydrate O-sulfate esters based on ab initio 6-31+ G** calculations on methyl and ethyl sulfate anions. *J. Am. Chem. Soc.* **1993**, *115*, 9648–9654.

(7) Alemán, C.; Zanuy, D.; Casanovas, J. A Quantum Mechanical Study on the Electrostratic Interactions of Poly(l-lysine)·Alkyl Sulfate Complexes. *J. Phys. Chem. A* **2003**, *107*, 4151–4156.

(8) Remko, M.; van Duijen, P. T.; von der Lieth, C. W. Structure and Stability of Li(I) and Na(I) Carboxylate, Sulfate and Phosphate Complexes. *J. Mol. Struc.: THEOCHEM* **2007**, *814*, 119–125.

(9) Muralidharan, A.; Pratt, L. R.; Chaudhari, M. I.; Rempe, S. B. Quasi-chemical theory for anion hydration and specific ion effects: Cl^-(aq) vs F^-(aq). *Chem. Phys. Lett.* **2019**, *4*, 100037.

(10) Chaudhari, M. I.; Vanegas, J. M.; Pratt, L. R.; Muralidharan, A.; Rempe, S. B. Hydration Mimicry by Membrane Ion Channels. *Ann. Rev. Phys. Chem.* **2020**, *71*, 461–484.

(11) Gomez, D.; Pratt, L. R.; Asthagiri, D. N.; Rempe, S. B. Hydrated anions: From clusters to bulk solution with quasi-chemical theory. *Acc. Chem. Res.* **2022**, *55*, 2201–2212.

(12) Stevens, M. J.; Rempe, S. L. B. Binding of Carboxylate and Water to Monovalent Cations. *Phys. Chem. Chem. Phys.* **2023**, *25*, 29881–29893.

(13) Rempe, S. B.; Pratt, L. R.; Hummer, G.; Kress, J. D.; Martin, R. L.; Redondo, A. The Hydration Number of Li^+ in Liquid Water. *J. Am. Chem. Soc.* **2000**, *122*, 966–967.

(14) Rempe, S. B.; Pratt, L. R. The Hydration Number of Na^+ in Liquid Water. Fl. Phase Eq. 2001; pp 121–132.

(15) Rempe, S. B.; Asthagiri, D.; Pratt, L. R. Inner Shell Definition and Absolute Hydration Free Energy of K^+(aq) on the Basis of Quasi-Chemical Theory and Ab Initio Molecular Dynamics. *Phys. Chem. Chem. Phys.* **2004**, *6*, 1966.

(16) Sabo, D.; Jiao, D.; Varma, S.; Pratt, L. R.; Rempe, S. B. Case Study of Rb^+(aq), Quasi-Chemical Theory of Ion Hydration, and the *No Split Occupancies* Rule. *Ann. Rep. Sec. "C" (Phys. Chem.)* **2013**, *109*, 266–278.

(17) Chaudhari, M. I.; Soniat, M.; Rempe, S. B. Octa-Coordination and the Aqueous Ba^{2+} Ion. *J. Phys. Chem. B* **2015**, *119*, 8746–8753.

(18) Chaudhari, M.; Rempe, S. B. Strontium and barium in aqueous solution and a potassium channel binding site. *J. Chem. Phys.* **2018**, *148*, 222831.

(19) Chaudhari, M. I.; Pratt, L. R.; Rempe, S. B. Utility of chemical computations in predicting solution free energies of metal ions. *Mol. Simul.* **2018**, *44*, 110–116.

(20) Soniat, M.; Rick, S. W. The effects of charge transfer on the aqueous solvation of ions. *J. Chem. Phys.* **2012**, *137*, 044511.

(21) Berkowitz, M. L. Molecular Simulations of Aqueous Electrolytes: Role of Explicit Inclusion of Charge Transfer into Force Fields. *J. Phys. Chem. B* **2021**, *125*, 13069–13076.

(22) Stevens, M. J.; Rempe, S. L. B. Binding of Li^+ to Negatively Charged and Neutral Ligands in Polymer Electrolytes. *J. Phys. Chem. Lett.* **2023**, *14*, 10200–10207.

(23) Herman, C. E.; Valiya Parambathu, A.; Asthagiri, D. N.; Lenhoff, A. M. Polarizability Plays a Decisive Role in Modulating Association between Molecular Cations and Anions. *J. Phys. Chem. Lett.* **2023**, *14*, 7020–7026.

(24) Varma, S.; Rempe, S. B. Tuning Ion Coordination Architectures to Enable Selective Partitioning. *Biophys. J.* **2007**, *93*, 1093–1099.

(25) Bostick, D.; Brooks III, C. L. Selectivity in K^+ Channels Is Due to Topological Control of the Permeant Ion's Coordinated State. *Proc. Natl. Acad. Sci. USA* **2007**, *104*, 9260 – 9265.

(26) Varma, S.; Rempe, S. B. Structural Transitions in Ion Coordination Driven by Changes in Competition for Ligand Binding. *J. Am. Chem. Soc.* **2008**, *130*, 15405–15419.

(27) Varma, S.; Sabo, D.; Rempe, S. B. $\mathrm{K}^+/\mathrm{Na}^+$ Selectivity in K Channels and Valinomycin: Over-Coordination Versus Cavity-Size Constraints. *J. Molec. Biol.* **2008**, *376*, 13–22.

(28) Asthagiri, D.; Dixit, P. D.; Merchant, S.; Paulaitis, M. E.; Pratt, L. R.; Rempe, S. B.; Varma, S. Ion Selectivity from Local Configurations of Ligands in Solutions and Ion Channels. *Chem. Phys. Lett.* **2010**, *485*, 1–7.

(29) Varma, S.; Rogers, D. M.; Pratt, L. R.; Rempe, S. B. Perspectives On: Ion Selectivity: Design Principles for K^+ Selectivity in Membrane Transport. *J. Gen. Phys.* **2011**, *137*, 479–488.

(30) Stevens, M. J.; Rempe, S. L. B. Ion-Specific Effects in Carboxylate Binding Sites. *J. Phys. Chem. B* **2016**, *120*, 12519–12530.

(31) Stevens, M. J.; Rempe, S. L. B. Carboxylate Binding Prefers Two Cations to One. *Phys. Chem. Chem. Phys.* **2022**, *24*, 22198–22205.

(32) Pratt, L. R.; Rempe, S. B. In *Simulation and Theory of Electrostatic Interactions in Solution, AIP Press, Vol. 492, New York*; Hummer, G., Pratt, L. R., Eds.; AIP Conf. Proc., 1999; Vol. 492; pp 172–201.

(33) Rogers, D. M.; Jiao, D.; Pratt, L. R.; Rempe, S. B. Structural Models and Molecular Thermodynamics of Hydration of Ions and Small Molecules. *Ann. Rep. Comp. Chem.* **2012**, *8*, 71.

(34) Chaudhari, M. I.; Rempe, S. B.; Pratt, L. R. Quasi-chemical theory of F^-(aq): The "no split occupancies rule" revisited. *J. Chem. Phys.* **2017**, *147*, 161728.

(35) Tomasi, J.; Mennucci, B.; Cammi, R. Quantum Mechanical Continuum Solvation Models. *Chem. Rev.* **2005**, *105*, 2999–3093.

(36) Frisch, M. J.; Trucks, G. W.; Schlegel, H. B.; Scuseria, G. E.; Robb, M. A.; Cheeseman, J. R.; Scalmani, G.; Barone, V.; Petersson, G. A.; Nakatsuji, H. et al. Gaussian 16 Revision C.01. 2016; Gaussian Inc. Wallingford CT.

(37) Rempe, S. B.; Jónsson, H. A Computational Exercise Illustrating Molecular Vibrations and Normal Modes. *Chem. Educ.* **1998**, *3*, 1–17.

(38) Chai, J.-D.; Head-Gordon, M. Long-range corrected hybrid density functionals with damped atom-atom dispersion corrections. *Phys. Chem. Chem. Phys.* **2008**, *10*, 6615–6620.

(39) Soniat, M.; Rogers, D. M.; Rempe, S. B. Dispersion- and Exchange-Corrected Density Functional Theory for Sodium Ion Hydration. *J. Chem. Theory Comput.* **2015**, 2958–2967.

(40) Seeger, Z. L.; Izgorodina, E. I. A Systematic Study of DFT Performance for Geometry Optimizations of Ionic Liquid Clusters. *J. Chem. Theory Comput.* **2020**, *16*, 6735–6753.

(41) Peterson, K. A.; Dunning, T. H. Accurate Correlation Consistent Basis Sets for Molecular Core–Valence Correlation Effects: The Second Row Atoms Al–Ar, and the First Row Atoms B–Ne Revisited. *J. Chem. Phys.* **2002**, *117*, 10548.

(42) Hill, J. G.; Peterson, K. A. Gaussian basis sets for use in correlated molecular calculations. XI. Pseudopotential-based and all-electron relativistic basis sets for alkali metal (K–Fr) and alkaline earth (Ca–Ra) elements. *J. Chem. Phys.* **2017**, *147*, 244106.

(43) Rogers, D. M.; Rempe, S. B. Probing the Thermodynamics of Competitive Ion Binding Using Minimum Energy Structures. *J. Phys. Chem. B* **2011**, *115*, 9116–9129.

(44) Sabo, D.; Varma, S.; Martin, M. G.; Rempe, S. B. Studies of the Thermodynamic Properties of Hydrogen Gas in Bulk Water. *J. Phys. Chem. B* **2008**, *867-876*.

(45) Leung, K.; Rempe, S. B.; von Lilienfeld, O. A. Ab initio molecular dynamics calculations of ion hydration free

energies. *J. Chem. Phys.* **2009**, *130*, 204507.

(46) Gomez, D. T.; Pratt, L. R.; Rogers, D. M.; Rempe, S. B. Free energies of hydrated halide anions: High throughput computations on clusters to treat rough energy-landscapes. *Molecules* **2021**, *26*, 3087.

(47) Mason, P. E.; Ansell, S.; Neilson, G.; Rempe, S. B. Neutron Scattering Studies of the Hydration Structure of Li^+. *J. Phys. Chem. B* **2015**, *119*, 2003–2009.

(48) Chaudhari, M.; Nair, J. R.; Pratt, L. R.; Soto, F. A.; Balbuena, P. B.; Rempe, S. B. Scaling Atomic Partial Charges of Carbonate Solvents for Lithium Ion (Li^+) Solvation and Diffusion. *J. Chem. Theory Comput.* **2016**, *12*, 5709–5718.

(49) Muralidharan, A.; Pratt, L. R.; Chaudhari, M. I.; Rempe, S. B. Comparison of single-ion molecular dynamics in common solvents. *J. Chem. Phys.* **2018**, *148*, 222821.

(50) Chaudhari, M. I.; Muralidharan, A.; Pratt, L. R.; Rempe, S. B. Assessment of simple models for molecular simulation of ethylene carbonate and propylene carbonate as solvents for electrolyte solutions. *Top. Current. Chem. (Z)* **2018**, *376*, 7.

(51) Humphrey, W.; Dalke, A.; Schulten, K. VMD – Visual Molecular Dynamics. *J. Molec. Graphics* **1996**, *14*, 33–38.

(52) Breneman, C.; Wiberg, K. Determining Atom-centered Monopoles from Molecular Electrostatic Potentials. the Need for High Sampling Density in Formamide Conformational Analysis. *J. Comp. Chem.* **2004**, *11*, 361–373.

(53) Leontyev, I.; Stuchebrukhov, A. Accounting for electronic polarization in non-polarizable force fields. *Phys. Chem. Chem. Phys.* **2011**, *13*, 2613–2626.

(54) Zeron, I. M.; Abascal, J. L. F.; Vega, C. A force field of Li^+, Na^+, K^+, Mg^{2+}, Ca^{2+}, Cl^- and SO_4^{2-} in aqueous solution based on the TIP4P/2005 water model and scaled charges for the ions. *J. of Chem. Phys.* **2019**, *151*, 134504.

(55) Dal Peraro, M.; Raugei, S.; Carloni, P.; Klein, M. L. Solute–Solvent Charge Transfer in Aqueous Solution. *ChemPhysChem* **2005**, *6*, 1715–1718.

(56) Marenich, A. V.; Olson, R. M.; Chamberlin, A. C.; Cramer, C. J.; Truhlar, D. G. Polarization Effects in Aqueous and Nonaqueous Solutions. *J. Chem. Theory Comput.* **2007**, *3*, 2055–2067.

(57) Kim, J. S.; Wu, Z.; Morrow, A.; Yethiraj, A.; Yethiraj, A. Self-Diffusion and Viscosity in Electrolyte Solutions. *J. Phys. Chem. B* **2012**, *116*, 12007–12013.

(58) Yao, Y.; Kanai, Y.; Berkowitz, M. L. Role of Charge Transfer in Water Diffusivity in Aqueous Ionic Solutions. *J. of Phys. Chem. Lett.* **2014**, *5*, 2711–2716.

(59) Yao, Y.; Berkowitz, M. L.; Kanai, Y. Communication: Modeling of concentration dependent water diffusivity in ionic solutions: Role of intermolecular charge transfer. *J. of Chem. Phys.* **2015**, *143*, 241101.

(60) Nadig, G.; Van Zant, L. C.; Dixon, S. L.; Merz, K. M. Charge-Transfer Interactions in Macromolecular Systems: A New View of the Protein/Water Interface. *J. Am. Chem. Soc.* **1998**, *120*, 5593–5594.

(61) Leontyev, I. V.; Vener, M. V.; Rostov, I. V.; Basilevsky, M. V.; Newton, M. D. Continuum Level Treatment of Electronic Polarization in the Framework of Molecular Simulations of Solvation Effects. *J. Chem. Phys.* **2003**,

119, 8024–8037.

(62) Berendsen, H. J. C.; Grigera, J. R.; Straatsma, T. P. The missing term in effective pair potentials. *J. Phys. Chem.* **1987**, *91*, 6269–6271.

(63) Jorgensen, W. L.; Chandrasekhar, J.; Madura, J. D.; Impey, R. W.; Klein, M. L. Comparison of simple potential functions for simulating liquid water. *J. Chem. Phys.* **1983**, *79*, 926–935.

TOC Graphic

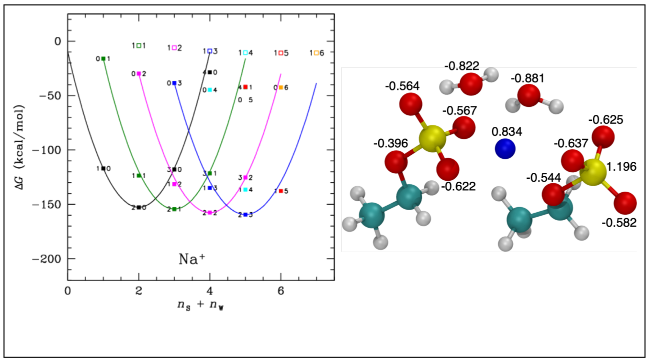
ΔG (kcal/mol)
0
−50
−100
−150
−200
0
2
4
6
$n_s + n_w$
Na⁺
1 1
1 2
1 3
1 4
1 5
1 6
0 1
0 2
4 0
0 3
0 4
4 1
0 6
0 5
1 0
1 1
3 0
3 1
3 2
1 2
1 3
1 4
1 5
2 0
2 1
2 2
2 3
-0.822
-0.881
-0.564
-0.567
0.834
-0.625
-0.396
-0.637
1.196
-0.544
-0.622
-0.582